

MECHANICAL PROPERTIES, PHYSICS OF STRENGTH, AND PLASTICITY

Electronic Structure of the Zr–He System

O. V. Lopatina^{a,*}, Yu. M. Koroteev^b, and I. P. Chernov^a

^a National Research Tomsk Polytechnic University, pr. Lenina 30, Tomsk, 634050 Russia

* e-mail: lopatina_oksana@tpu.ru

^b Institute of Strength Physics and Materials Science, Siberian Branch of the Russian Academy of Sciences,
pr. Akademicheskii 2/4, Tomsk, 634021 Russia

Received June 3, 2013; in final form, October 20, 2013

Abstract—Ab initio calculations of the electronic structure of the HCP and FCC zirconium with impurity of helium atoms of about 6% have been performed. It has been established that the presence of helium noticeably varies the electronic structure of Zr and leads to considerable redistribution of its electron density. Calculated values of chemical shifts of skeleton states of Zr atoms caused by the presence of helium atoms in its lattice have been discussed.

DOI: 10.1134/S1063783414050151

1. INTRODUCTION

During the operation of nuclear and thermonuclear reactors, construction materials of their elements accumulate impurity helium atoms and numerous defects of both the thermal and radiation nature. This circumstance negatively affects the radiation resistance of materials and becomes the cause of catastrophic worsening their properties, which shortens the service life of constructive elements of reactors. Negative consequences of accumulation of helium are radiation swelling, high-temperature and low-temperature radiation embrittlement, radiation creep, etc. [1, 2]. When studying these phenomena, the main attention was paid to studying the behavior of the atomic subsystem of materials. Results of numerous publications in this branch are generalized in monographs and reviews [1–6]. A weak point of such approach is underestimation of the role of the electron subsystem of materials when analyzing the above-described phenomena. To date, there are few publications devoted to studying the electronic structure of metal–helium systems [7–12]. However, the authors of [12] showed based on ab initio calculations what a high concentration of helium atoms (~30 at %) in the Zr lattice leads to a considerable variation not only in atomic but also in the electronic structure of metal. As for relatively low helium concentration, we should expect that the atomic subsystem of metal would be perturbed somewhat weaker, although its electronic structure can change noticeably.

This study is devoted to the investigation into the electronic structure of the Zr–He system with the tetrahedral and octahedral coordination of the helium atom in the HCP and FCC lattices of metal at its concentration of ~6 at %. We investigated the variations in the density of electron states and spatial distributions of the charge density of metal as well as analyzed

chemical shifts of skeleton Zr levels due to the incorporation of He.

2. DETAILS OF THE CALCULATION

Self-consistent calculations of the electronic structure of pure Zr and the Zr–He system with the impurity concentration of ~6 at % were performed in the context of the electron density functional theory using the generalized-gradient approximation [13] by the linearized method of attached plane waves [14, 15] implemented in the FLEUR software package. Densities of electron states (DES) were calculated by the linear method of tetrahedrons for the network of 54 k points in the irreducible part of the Brillouin zone (IPBZ) of HCP and FCC lattices. DES was smoothed by Gaussians with the mean-root-square width of 0.13 eV. Radii of muffin-tin (MT) spheres of Zr and He atoms were selected equal to 2.3 and 1.0 a.u. (atomic units), respectively. The used parameter of cutting the basis of plane waves $k_{\max} = 4.0 \text{ a.u.}^{-1}$ corresponded to ~170 basis functions per atom. Eigenvalues of the Hamiltonian were calculated in 14 k points of the IPBZ of the HCP structure and in 10 k points of the IPBZ of the FCC structure at each self-consistency iteration. The self-consistency procedure of the electron density was performed until the convergence of the total energy no worse than 0.001 meV, which corresponded to convergence of the charge density no worse than $1 \times 10^{-7} \text{ e/a.u.}^3$, was attained. Computational cells for pure Zr contained 16 atoms and for the Zr–He system, they additionally contained one helium atom.

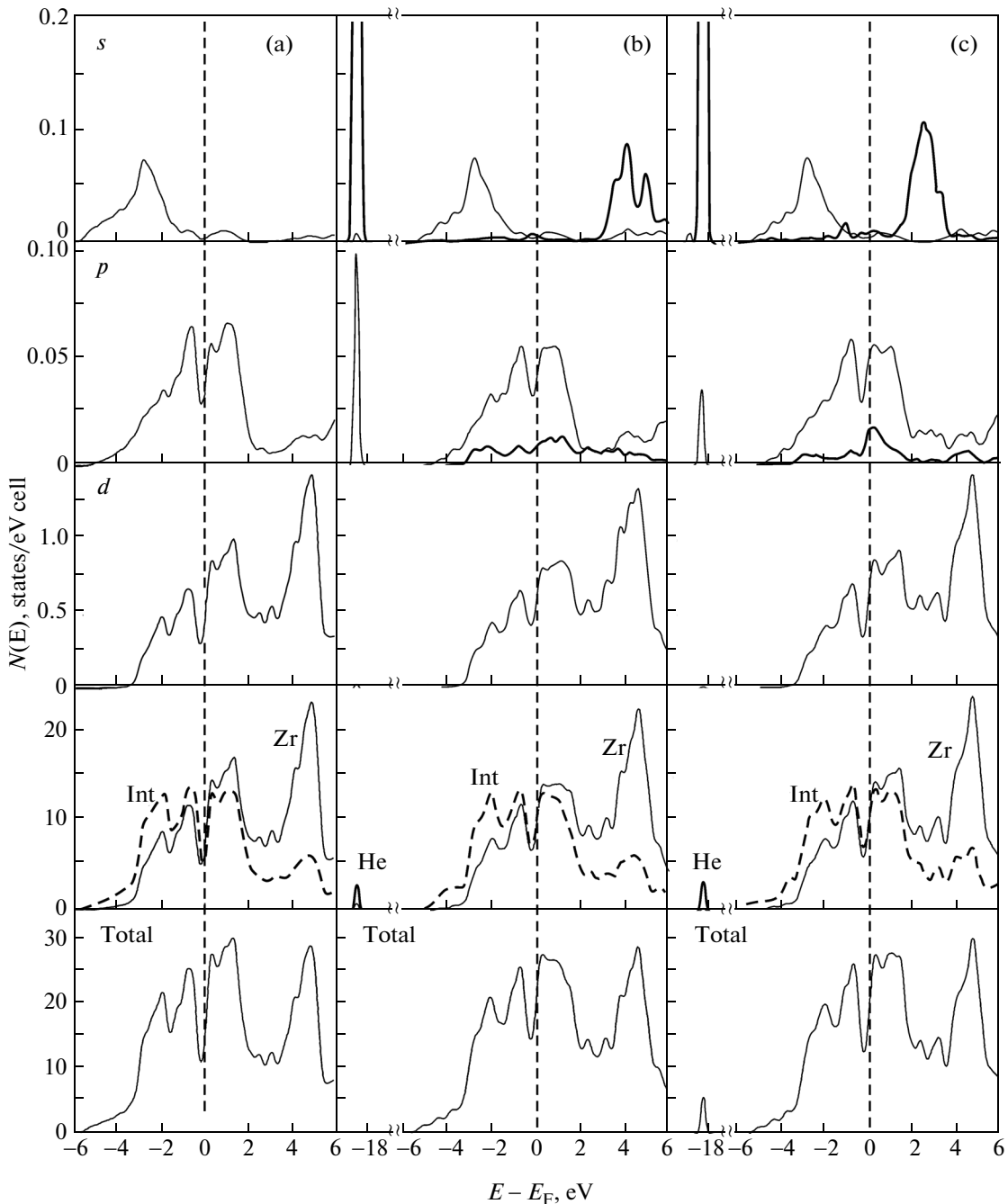


Fig. 1. Density of electron states $N(E)$ of (a) pure HCP Zr and the Zr–He system with (b) tetrahedral and (c) octahedral coordination of the He atom in the HCP lattice of metal. The total density of electron states (Total), the local density of electron states in the interatomic region (Int) and in MT spheres of zirconium and helium atoms as well as partial densities of states of s , p , and d type are shown.

3. RESULTS AND DISCUSSION

It is known that pure zirconium has the HCP structure under standard conditions. Our calculations of the total energy of the Zr–He system showed that in the presence of ~ 6 at % helium impurity, the HCP lattice of Zr remains most stable among all ones that can occur for this metal. It is also found that with the He

concentration under consideration, the FCC lattice of Zr with the helium atom in the octahedral interstice can be implemented. The difference of total energies of HCP and FCC lattices of He with the helium atom in the octahedral interstice was ~ 0.001 eV/atom by the results of our calculations. Starting from this fact, we selected three systems as the objects for investigations: the HCP zirconium with the octahedral and tetrahe-

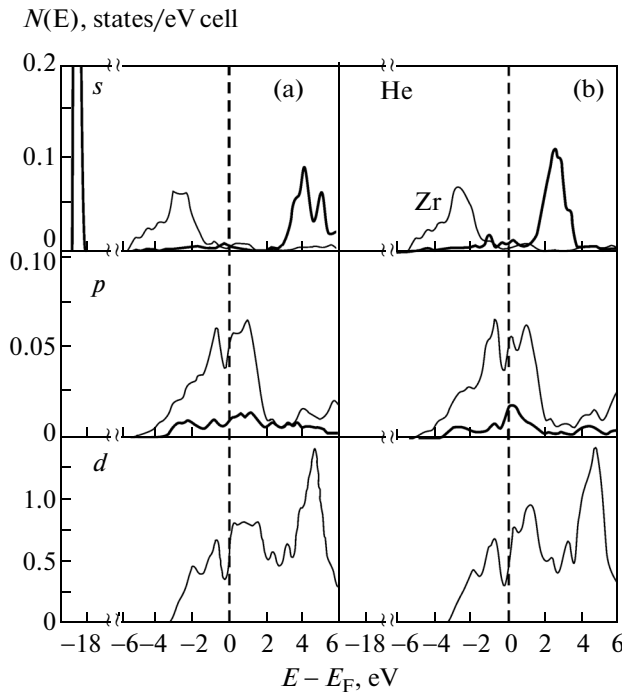


Fig. 2. Local partial densities of states of s , p , and d type in MT spheres of the He atom and HCP Zr atoms of the second coordination sphere of the helium atom with the (a) tetrahedral and (b) octahedral coordination.

dral site of helium as well as FCC Zr with the He atom in the octahedral interstice.

Density of Electron States

Our calculated DES curves for pure HCP Zr and the Zr–He for various sites of helium atoms in the FCC lattice of metal are shown in Fig. 1. It is seen that the results found for pure metal agree well with the data of studies [16, 17]. We can conclude from the analysis of the total DES that the following occurs due to the incorporation of helium into the tetrahedral pore and octahedral pore of the metal lattice:

(i) a narrow (~ 1.0 eV wide) band of s states of He separated from valence states of metal by a gap of ~ 12.0 eV appears below the conduction band bottom;

(ii) the width of the conduction band of Zr decreases by approximately 0.2 eV;

(iii) DES at the Fermi level of systems with the tetrahedral and octahedral coordination of helium atoms increases by approximately 5.5 states/eV cell relative to DES for pure zirconium. The last circumstance indicates the higher degree of metallicity of the Zr–He system compared with pure Zr.

It is seen from the analysis of local DESs that the larger part of the valent charge density of metal is located in the interatomic region. Our calculations show that the incorporation of helium increases the valent charge in the interatomic region of the compu-

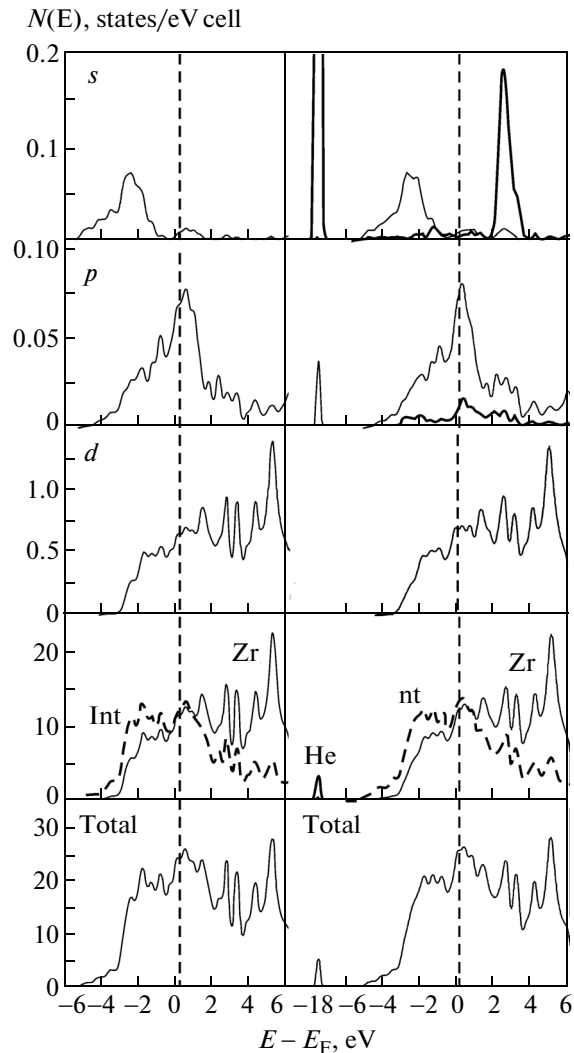


Fig. 3. Density of electron states $N(E)$ of (a) pure FCC Zr and (b) the Zr–He system with the octahedral coordination of the He atom in the HCP lattice of metal. Notation is the same as in Fig. 1.

tational cell by $0.75e$. An increase in lattice parameters of Zr, which is caused by the incorporation of helium, leads to a decrease in the valent charge in MT spheres of metal by $0.02e$. The valent charge in MT spheres of Zr atoms nearest to the helium atom (atoms of the first coordination sphere) increases by $0.05e$ at the background of this decrease.

It is also seen from Fig. 1 that the presence of helium atoms noticeably varies partial DESs in MT spheres of Zr nearest to the helium atom. For example, a considerable p -type peak caused by the propagation of “tails” of $1s$ state of helium into the MT sphere of metal appears in the vicinity of energy of ~ -19 eV. It is noteworthy that partial DESs of zirconium atoms arranged in the second coordination sphere of helium (Fig. 2) do not contain this peak. The p states, which are apparently the “tails” of d states of Zr atoms, are

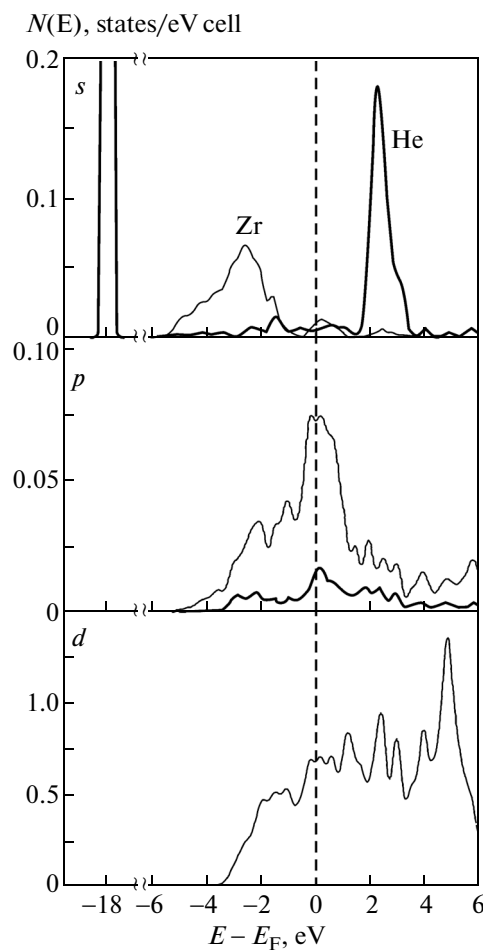


Fig. 4. Local partial densities of states of s , p , and d type in MT spheres of the He atom and FCC Zr atoms of the second coordination sphere of the helium atom with the octahedral coordination.

observed in the energy region from -6.0 to 3.0 eV in the MT sphere of helium. The DES peak generated by $2s$ states of helium is present above 3.0 eV in MT sphere of helium.

Figures 3 and 4 shows DES curves for pure FCC Zr and the Zr–He system with the octahedral arrangement of helium atoms in the FCC lattice of metal. It is seen that the impurity changes the electronic structure of the FCC metal similarly to the case of the HCP lattice. The only difference is that the width of the conduction band of Zr decreases by 0.16 eV, while its DES at the Fermi level increases by 1.3 states/eV cell.

Charge Density

We calculated spatial distributions of the charge density for pure Zr and the Zr–He as well as their difference for some crystallographic planes. Figure 5 shows the computational cell of the HCP structure of the Zr–He system and three planes p_1 , p_2 , and p_3 that we considered, which are parallel to base plane (0001)

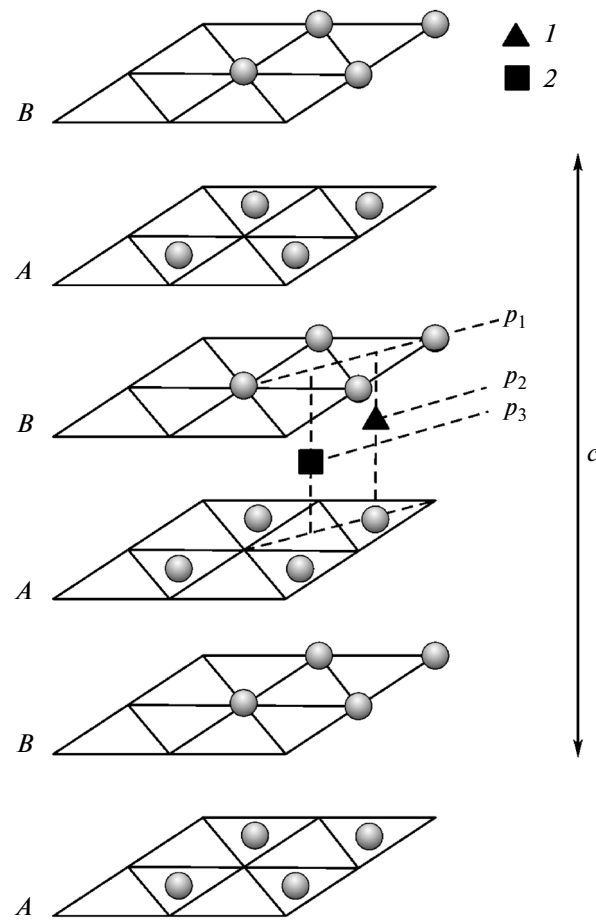


Fig. 5. Computational cell of the HCP structure of the Zr–He system. A and B are the closely packed layers of the HCP lattice of Zr and (1, 2) are the tetrahedral and octahedral interstices, respectively; and c is the parameter of the computational cell along axis z .

of the HCP structure. Figures 6 and 7 represent the distributions of the charge density of pure Zr and the Zr–He system in the HCP structure with the tetrahedral and octahedral coordination of the impurity helium atom. Figures 6a, 6d, 6g, 6j; 6b, 6e, 6h, 6k; and 6c, 6f, 6i, 6l show charge densities in planes p_1 , p_2 , and p_3 , respectively. Figure 6e represents the sites of helium atoms as well as the projections of sites of zirconium atoms of the first and second coordination spheres. Figures 7a, 7c, 7e and 7b, 7d, 7f show charge densities in planes p_1 and p_3 , respectively. Figure 7b shows the sites of zirconium atoms of the first and second coordination spheres as well as the projection of the site of the helium atom. It is seen from the analysis of the results presented in Figs. 6a–6f and 7a, 7b that the incorporation of helium causes a noticeable variation in the charge density of the system. To analyze this variation in more detail, Figs. 6g–6i and 7c, 7d represent the negative values of the difference of densities $\Delta\rho(r) = \rho_{\text{Zr-He}}(r) - \rho_{\text{Zr}}(r) - \rho_{\text{He}}(r)$, while Figs. 6j–6l and 7e, 7f represent the positive ones. It is seen from

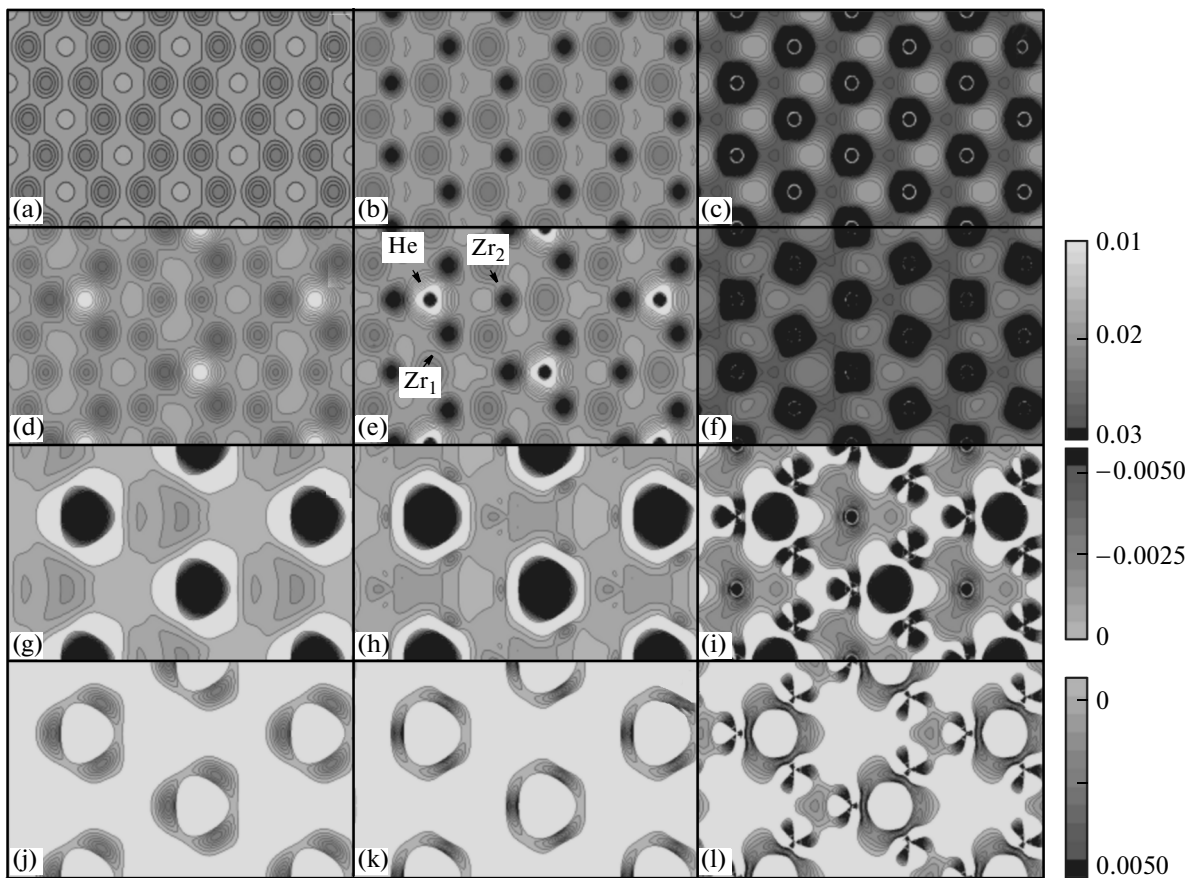


Fig. 6. Distribution of charge density $\rho(r)$ of the HCP structure of pure Zr and the Zr–He system with the tetrahedral coordination of the He atom. (a–c) Charge densities $\rho_{\text{Zr}}(r)$ of pure Zr, (d–f) charge densities $\rho_{\text{Zr}-\text{He}}(r)$ of the Zr–He system, and (g–i) negative and (j–l) positive values of the difference of valent densities $\Delta\rho(r)$.

Figs. 6g–6i and 7c, 7d that entering the tetrahedral or octahedral interstice of the HCP lattice of Zr, helium forces out electrons of metal from there and leads to a decrease in the charge density in MT spheres of Zr atoms of the second coordination sphere and in the interatomic space surrounding them. A significant nonuniformity of redistribution of the charge density is observed in MT spheres of Zr atoms of the first coordination sphere. It is seen from Figs. 6j–6l and 7e, 7f that an increase in the charge density occurs mainly in the region of the first coordination sphere of the helium atom.

Figure 8 shows the charge density distribution of the FCC structure of pure Zr and the Zr–He system with the octahedral coordination of the helium atom calculated in the plane passing both Zr atoms and He atoms. Figure 8b shows the sites of the helium atom and zirconium atoms of the first coordination sphere as well as projections of sites of Zr atoms of the second coordination sphere. It is seen from Figs. 8a and 8b that the incorporation of helium causes a noticeable redistribution of the charge density of the system. Figures 8c and 8d represent the negative and positive differences of densities $\Delta\rho(r)$, respectively. It is seen that

entering the octahedral interstice of the FCC lattice of Zr (Fig. 8c), the helium atom forces out electrons of metal from the region occupied by them and leads to a decrease in the charge density in octahedral interstices nearest to it. A very large redistribution nonuniformity of the charge density is observed in MT spheres of Zr atoms of the first coordination sphere. Fig. 8d shows that an increase in the charge density occurs mainly in the region of the first coordination sphere of the helium atom and in empty octahedral interstices of the second coordination sphere.

Skeleton Shifts

Binding energies of skeleton levels of components of various compounds are widely used to interpret the results of physicochemical processes [18–22]. These energies are determined experimentally using X-ray photoemission spectroscopy (XPES) or other spectroscopic methods. The set of binding energies specific for each atom makes it possible to determine the chemical composition of the material, and we can judge the chemical state of atoms and their site in the lattice of the host substance by the shift of skeleton lev-

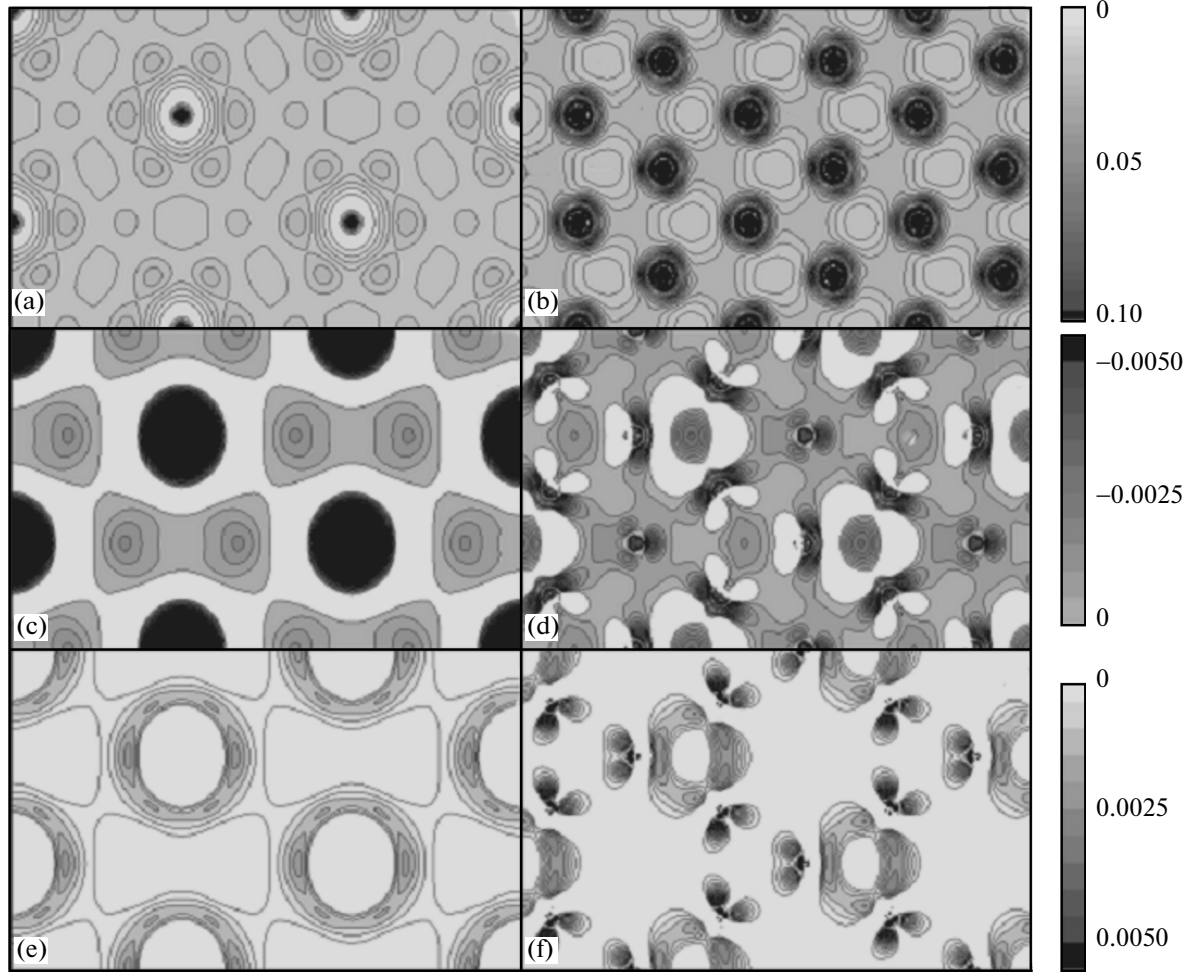


Fig. 7. Distribution of charge density $\rho(r)$ of the HCP structure of the Zr–He system with the octahedral coordination of the helium atom. (a, b) Charge densities $\rho_{\text{Zr-He}}(r)$ of the Zr–He system, and (c, d) negative and (e, f) positive values of the difference of valent densities $\Delta\rho(r)$.

els since the variation in the electron state of the atom upon its incorporation into the crystal changes the energies of even deeper levels [23].

In this study, we calculated in a self-consistent manner not only the energy spectra of valent electrons of pure Zr and the Zr–He system but also the energies of skeleton levels of metal atoms. This allowed us to calculate chemical shifts δE^{Zr} of skeleton states of Zr atoms caused by the presence of helium in the metal lattice. The magnitude of these shifts was determined as the difference

$$\delta E^{\text{Zr}} = E_{\text{Zr-He}}^{\text{Zr}} - E_{\text{Zr}},$$

where $E_{\text{Zr-He}}^{\text{Zr}}$ and E_{Zr} are the energies of skeleton levels of Zr atoms of the Zr–He system and pure metal, respectively. Table 1 represents the energies of skeleton levels of Zr atoms in the HCP lattice of the Zr–He system and pure metal as well as the shifts of these levels caused by the incorporation of helium atoms. Digits 1

and 2 denote the types of Zr atoms of the first coordination sphere of He. First-type atoms are arranged in a vertex of impurity-containing tetrahedron, while second-type atoms form its basis. It is seen from Table 1 that due to the incorporation of helium atoms, skeleton levels of Zr atoms are shifted to higher binding energies (all skeleton shifts have negative values). In the case of the tetrahedral site of the helium atom, the magnitude of skeleton shifts for the first-type Zr atoms has values in a range from -0.25 to -0.27 eV, and only $4s$ state shifts by -0.36 eV. Shifts for second-type atoms lie in a range from -0.033 to -0.35 eV. With the octahedral coordination of the He atom, skeleton shifts for the first-type Zr atoms lie in a range of approximately from -0.16 to -0.18 eV, while for the second-type atoms—in a range from -0.13 to -0.15 eV. Skeleton shifts for Zr atoms of the second coordination sphere in the case of the tetrahedral coordination of the He atom lie in ranges $(-0.28, -0.30)$ and $(-0.31, -0.34)$ eV, while for the octahedral coordination—in ranges

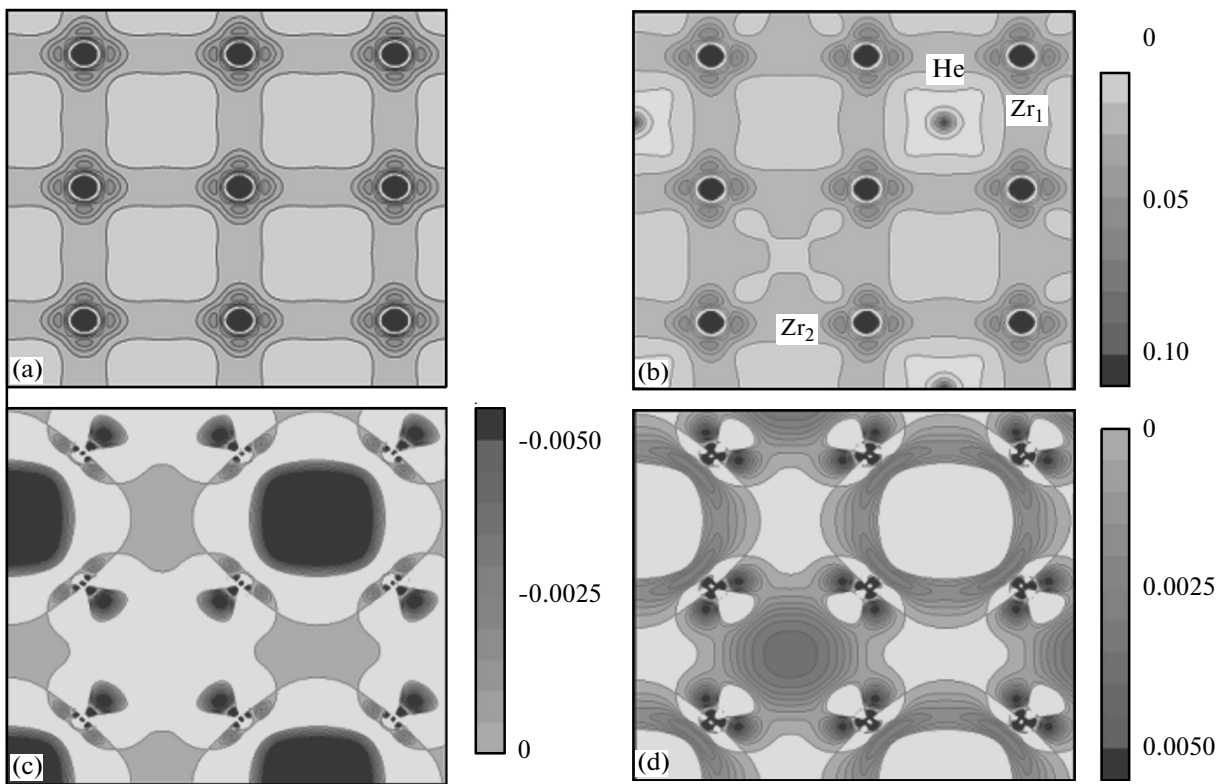


Fig. 8. Distribution of charge density $\rho(r)$ of the FCC structure of (a) pure Zr and (b) the Zr–He system with the octahedral coordination of the helium atom; (c) negative and (d) positive values of the difference of valent densities $\Delta\rho(r)$.

(−0.13, −0.15) and (−0.15, −0.17) eV for the first-type and second-type atoms, respectively.

Table 2 represents the data for the FCC structure similar to those presented in Table 1. Similarly to the previous case, digits 1 and 2 denote types of Zr atoms.

Table 1. Energies of skeleton levels of Zr atoms in HCP lattices of the Zr–He system and pure metal as well as the shifts of these levels caused by the presence of He atoms

Skeleton level	$E_{\text{Zr-He}}^{\text{Zr}}$, eV				E_{Zr} , eV	δE^{Zr} , eV				
	Tetra		Octa			Tetra		Octa		
	1	2	1	2		1	2	1	2	
$1s^2$	−17800.2863	−17800.3679	−17800.2047	−17800.1720	−17800.027	−0.2593	−0.3409	−0.1777	−0.1450	
$2s^2$	−2451.3348	−2451.4083	−2451.2586	−2451.2096	−2451.079	−0.2558	−0.3293	−0.1796	−0.1306	
$2p^2$	−2242.4629	−2242.5364	−2242.3840	−2242.3378	−2242.207	−0.2559	−0.3294	−0.1770	−0.1308	
$2p^4$	−2156.6219	−2156.6954	−2156.5430	−2156.4967	−2156.366	−0.2559	−0.3294	−0.1770	−0.1307	
$3s^2$	−367.5962	−387.6533	−387.4955	−387.4547	−387.321	−0.2752	−0.3323	−0.1745	−0.1337	
$3p^2$	−309.8478	−309.9050	−309.7444	−309.7036	−309.570	−0.2778	−0.3350	−0.1744	−0.1336	
$3p^4$	−296.1823	−296.2394	−296.0816	−296.0408	−295.907	−0.2753	−0.3324	−0.1746	−0.1338	
$3d^4$	−159.1457	−159.2056	−159.0478	−159.0042	−158.871	−0.2747	−0.3346	−0.1768	−0.1332	
$3d^6$	−156.6505	−156.7076	−156.5498	−156.5062	−156.375	−0.2755	−0.3326	−0.1748	−0.1312	
$4s^2$	−37.7095	−37.6986	−37.5027	−37.4918	−37.345	−0.3645	−0.3536	−0.1577	−0.1468	

Tetra is the tetrahedral coordination of the helium atom in the HCP lattice of Zr and octa is the octahedral coordination of the helium atom in the HCP lattice of Zr.

Table 2. Energies of skeleton levels of Zr atoms in FCC lattices of the Zr–He system and pure metal as well as the shifts of these levels caused by the presence of He atoms

Skeleton level	$E_{\text{Zr-He}}^{\text{Zr}}$, eV		E_{Zr} , eV	δE^{Zr} , eV		
	Octa			Octa		
	1	2		1	2	
$1s^2$	−17800.1829	−17800.1747	−17799.886	−0.2969	−0.2887	
$2s^2$	−2451.2178	−2451.2096	−2450.932	−0.2858	−0.2776	
$2p^2$	−2242.3459	−2242.3378	−2242.057	−0.2889	−0.2808	
$2p^4$	−2156.5076	−2156.4995	−2156.219	−0.2886	−0.2805	
$3s^2$	−387.4629	−387.4547	−387.172	−0.2909	−0.2827	
$3p^2$	−309.7118	−309.7063	−309.423	−0.2888	−0.2833	
$3p^4$	−296.0489	−296.0408	−295.758	−0.2909	−0.2828	
$3d^4$	−159.0124	−159.0042	−158.724	−0.2884	−0.2802	
$3d^6$	−156.5144	−156.5090	−156.226	−0.2884	−0.2830	
$4s^2$	−37.4972	−37.4891	−37.198	−0.2992	−0.2911	

Octa is the octahedral coordination of the helium atom in the HCP lattice of Zr.

With the octahedral coordination of the He atom, skeleton shifts for the first-type and second-type Zr atoms have close values lying in a range from −0.28 to −0.30 eV. Magnitudes of skeleton shifts for the atoms of the second coordination sphere lie in ranges (−0.24, −0.26) and (−0.27, −0.29) eV for the first-type and second-type atoms, respectively.

Thus, we can see that the shifts of skeleton levels of Zr noticeably depend on the site of the helium atom in the HCP lattice of metal. With the tetrahedral site of the impurity, these shifts are twofold larger than for the octahedral site. Measuring these shifts experimentally, we can judge the impurity site in the HCP lattice of metal. In addition, occurring differences in the magnitude and character of skeleton shifts for two crystalline structures that we considered should be noted. For example, skeleton shifts for the octahedral site of the helium atom in FCC and HCP lattices differ from one another more than by a factor of 1.5 (−0.28 eV against −0.17 eV). In the case of the tetrahedral site of He in the HCP lattice, the difference is in the character of the shifts. With the tetrahedral site of He, skeleton shifts have two characteristic values −0.26 and −0.34 eV. As for the octahedral site, skeleton shifts are characterized by the value of −0.28 eV. This fact in totality with the photoemission data can allow us to judge the presence of regions (grains) in Zr crystals having different crystalline structure due to the implantation of helium.

4. CONCLUSIONS

Thus, the self-consistent calculation of the electronic structure of pure zirconium and the Zr–He system was performed in terms of the density functional

theory. Densities of electron states are calculated both for pure metal and for metal with impurity. It is shown that the states lying below the valence band bottom, which are localized at the He atom, occur in the electron spectrum of the Zr–He system. It is found that the incorporation of helium leads to an increase in the density of electron states of metal at the Fermi level. The analysis of calculated distributions of the charge density showed that entering the zirconium crystal, the helium atom causes considerable anisotropic redistribution of electron density of metal. Chemical shifts of skeleton states of Zr atoms caused by the presence of He in the metal lattice are calculated. These data in combination with the XPES data can be used to determine the site of helium atoms in the zirconium lattice.

ACKNOWLEDGMENTS

This study was supported by the Ministry of Education and Science of the Russian Federation in frameworks of the Program “Development of the Scientific Potential of the Higher School”.

REFERENCES

1. V. F. Zelenskii, I. M. Neklyudov, and T. P. Chernyaeva, *Radiation Defects and Swelling of Metals* (Naukova Dumka, Kiev, 1988) [in Russian].
2. A. G. Zaluzhnyi, Yu. N. Sokurskii, and V. N. Tebus, *Helium in Reactor Materials* (Energoatomizdat, Moscow, 1988) [in Russian].
3. H. Ullmaier, Radiat. Eff. **78**, 1 (1983).
4. H. Ullmaier, Nucl. Fusion **24**, 1039 (1984).
5. A. I. Ranyuk and V. F. Rybalko, *Helium in Metal Gratings: A Review* (Central Scientific Research Institute of

- Management, Economics and Information of Ministry for Atomic Energy of the Russian Federation (TSNII-ATOMINFORM), Moscow, 1986) [in Russian].
6. I. M. Neklyudov, V. F. Rybalko, and G. D. Tolstolutskaya, *Evolution of Distribution Dependences of Helium and Hydrogen in Materials in Processes of Irradiation and Annealing: A Review* (Central Scientific Research Institute of Management, Economics and Information of Ministry for Atomic Energy of the Russian Federation (TSNIIATOMINFORM), Moscow, 1985) [in Russian].
 7. T. Seletskaia, Y. Osetsky, R. E. Stoller, and G. M. Stoks, *Phys. Rev. Lett.* **94**, 046403 (2005).
 8. T. Seletskaia, Y. Osetsky, R. E. Stoller, and G. M. Stoks, *Phys. Rev. B: Condens. Matter* **78**, 134103 (2008).
 9. X. T. Zu, L. Yang, F. Gao, S. M. Peng, H. L. Heinisch, X. G. Long, and R. J. Kurtz, *Phys. Rev. B: Condens. Matter* **80**, 054104 (2009).
 10. L. Yang, S. M. Peng, X. G. Long, F. Gao, H. L. Heinisch, R. J. Kurtz, and X. T. Zu, *J. Phys.: Condens. Matter* **23**, 035701 (2011).
 11. L. Yang, S. M. Peng, X. G. Long, F. Gao, H. L. Heinisch, R. J. Kurtz, X. T. Zu, *J. Appl. Phys.* **107**, 054903 (2010).
 12. Yu. M. Koroteev, O. V. Lopatina, and I. P. Chernov, *Phys. Solid State* **51** (8), 1600 (2009).
 13. J. P. Perdew, K. Burke, and M. Ernzerhof, *Phys. Rev. Lett.* **77**, 3865 (1996).
 14. E. Wimmer, H. Krakauer, M. Wienert, and A. J. Freeman, *Phys. Rev. B: Condens. Matter* **24**, 864 (1981).
 15. M. Wienert, E. Wimmer, and A. J. Freeman, *Phys. Rev. B: Condens. Matter* **26**, 4571 (1982).
 16. *Calculated Electronic Properties of Ordered Alloys: A Handbook: The Elements and Their 3d/3d and 4d/4d Alloys*, Ed. by V. L. Moruzzi and C. B. Sommers (World Scientific, Singapore, 1995).
 17. G. B. Grad, P. Blacha, J. Luitz, and K. Schwarz, *Phys. Rev. B: Condens. Matter* **62**, 12743 (2000).
 18. T. S. Zyubina, A. S. Zyubin, L. V. Yashina, and V. I. Shtanov, *Russ. J. Inorg. Chem.* **53** (5), 752 (2008).
 19. M. V. Gomoyunova and I. I. Pronin, *Tech. Phys.* **49** 10, 1249 (2004).
 20. A. S. Zyubin, S. N. Dedyulin, L. V. Yashina, and V. I. Shtanov, *Russ. J. Inorg. Chem.* **52** (2), 242 (2007).
 21. A. S. Zyubin, S. N. Dedyulin, L. V. Yashina, and V. I. Shtanov, *Russ. J. Inorg. Chem.* **54** (5), 727 (2009).
 22. L. A. Pesin, I. V. Voinkova, S. E. Evsyukov, I. V. Gribov, V. L. Kuznetsov, and N. A. Moskina, *Izv. Chelyab. Nauchn. Tsentr. No. 4*, 21 (2004).
 23. K. Siegbahn, C. Nordling, A. Fahlman, R. Nordberg, K. Hamrin, J. Hedman, G. Johansson, T. Bergmark, S.-E. Karlsson, I. Lindgren, and B. Lindgren, *ESCA: Atomic, Molecular and Solid State Structure Studied by Means of Electron Spectroscopy* (Almqvist and Wiksell, Uppsala, Sweden, 1967; Mir, Moscow, 1971).

Translated by N. Korovin

SPELL: OK